Journal of Mechanics Engineering and Automation 7 (2017) 132-144
doi: 10.17265/2159-5275/2017.03.003

Passive Velocity Field Control of a Redundant Cable-Driven Robot with Tension Limitations

CAO Sheng, LUO Zhiwei and QUAN Changqin

Graduate School of System Informatics, Kobe University, 1-1 Rokkodai-cho, Nada-ku, Kobe 657-8501, Japan

Abstract: This paper proposes a novel dynamic control approach for a cable-driven robot with high redundant actuation and cable tension limitations to perform tracking task while interacting with environment. In order for a cable-driven exoskeleton robot to execute the task smoothly and safely, it is necessary to consider the tracking motion performance as well as passivity when interacting with the environment under the conditions of the actuation cables' redundancy and the pulling limitation. With the additional consideration of the maximum limitation of the cable tension, cable-driven robot actually can only apply a certain range of feasible wrench on the external environment, which makes the task executed by robot be restricted. In order to make designed wrench be feasible and keep the desired trajectory tracking ability, we present a new control method by extending PVFC (passive velocity field control) method considering tracking stability and passivity. The approach augmented a higher dimensional virtual flywheel dynamics in a specific orthogonal complement space of the cable's actuation space. After the final adjustment of the designed wrench with respect to the cable's constraint, this method is capable of driving the cable robot to complete the trajectory tracking task and realize the passivity.

Key words: Passivity, impedance control, model uncertainties.

1. Introduction

In recent years, researches on cable-driven robot have been attracted many attentions. This kind of the robot system utilizes cables to drive the moving platform that brings some merits including:

(1) Lightweight,

(2) Reduced end-effector inertial as compared with rigid arms,

(3) Ease of transportation and reconfiguration, and most importantly,

(4) Make it easy to fit with the complex biomechanical joint structures and so on.

These merits let the cable-driven robot be utilized on many aspects such as cable-driven rehabilitation exoskeleton robots.

Similar with the muscular system, cable-driven robots have two important characteristics:

(1) Cable has an inability that it can only actuate robots with positive tension force but not push.

(2) In order to make the system completely restrained, it is necessary to add the redundant cables into the system.

For example, the *m* degree of freedom system driven by *n* cables is completely restrained when $n \geq m+1$.

In fact, lacking of the compression ability of the cables makes the analysis be complicated and causes the difficulty of building control scheme of the system. Since this critical property, only those pose (positions and orientations) where cables in tension are reachable. The set of these poses can be classified as the feasible workspace. Since cable-driven robot has the inability of pushing, the analysis of the feasible workspace, which is quite important for the control of the cable-driven robot, becomes difficult. Alp et al. [1] classified the SEW (static equilibrium workspace) as the set of the poses can be attained statically considering the gravity. However, in other researches [2, 3], the set of the poses where cable tensions can

Corresponding author: CAO Sheng, Ph.D., research fields: robot's manipulator control, rehabilitation robot, cable-driven robot.

sustain an arbitrary external wrench acted at the robot is defined as the WCW (wrench closure workspace). Another important type of the identification of the feasible workspace is the wrench feasible workspace [4, 5], which represents the set of the poses where cable tensions can exert any bounded wrench of the specified set.

The push inability problem of the cable also impacts the construction of cable-driven robot's control scheme. Oh and Agrawal [6] proposed a method which handles the nonnegative control input problem of the cable-driven robot using both LP and QP programming solver. Fang et al. [7] suggested a method of using PD control law to control the motion of cable-driven robot considering the optimal tension distribution. However, the admissible zone mentioned in this research paper may not exist in some situations, which makes computer unable to complete the calculation of the tension distribution.

As we know, in order to optimally build the control scheme of the cable-driven robot, tension distribution problem is required to be considered. Traditional solution, like aforementioned research [6], used the traditional LP and QP programming to compute the one-norm (for example: the sum of all tension) or two-norm minimal tension distribution. Whereas, the usage of these linear programming brings some drawbacks such as the long computation time. Borgstrom et al. [8] proposed a method which introduces a slack variable to enable the explicit computation of the near-optimal feasible start point leading to the rapid calculation of tension distribution. This research also contributes to the computation of the optimally safe tension distribution which represents the tensions that are not closed to the minimal limit of the constraint after optimization.

Although tension distribution enables the robot to complete the desired task with the wrench in the specified set, some complicated tasks (such as tracking of the far desired position or the time-varying trajectory) would make the desired wrench out of the limitation so as the robot is unable to handle the task.

Oh and Agrawal [9] have attempted to build iterative computational framework which first calculates the reachable domain based on the initial position considering the nonnegative tension input constraint and then determines the most appropriate desired position which is the closest one toward to the final desired position in this feasible domain. Actually, in this fantastic work, the position tracking task of the cable-driven robot has been divided into a sequence of subtasks for the sake of the generation of the nonnegative tension. However, the algorithm proposed in this research is complicated to calculate the feasible domain and nonnegative tension. Moreover, the computation difficulty would increase fast along with the augment of the cable's quantity. This research also left the problem that final desired position moves in a trajectory out of account.

In this paper, we present a novel dynamic control method for cable-driven robot considering how to track the desired trajectory and to keep passivity. Compared with the previous method handling the position control of the cable-driven robot by considering the complex planning of the objective target positions, we enable the tracing of the desired velocity vector field in a work space. Moreover, in order to handle the safety problem of the robot when interacting with environment such as human, we further choose the method to realize the passivity. We augment the system for easy transferring of tension constraint to the wrench space and contribute to the feasible wrench design based on the transferred condition.

The paper is organized as following. Section 2 describes the problem formulation, and analyzes some previous methods. Section 3 presents our method of high dimension PVFC (passive velocity field control) of the cable driven robot. Section 4 is the conclusion of the whole paper.

2. Problem Formulation

In this section, we first describe the dynamics and the constrain conditions of the cable driven robot and review the previous proposed control approaches.

2.1 Dynamics of a Cable-Driven Robot

The dynamics of a robot manipulator interacting with its environment can be denoted as

$$\boldsymbol{M}(\boldsymbol{q})\ddot{\boldsymbol{q}} + \boldsymbol{C}(\boldsymbol{q},\dot{\boldsymbol{q}})\dot{\boldsymbol{q}} = \boldsymbol{\tau} + \boldsymbol{J}^{\boldsymbol{T}}\boldsymbol{f} \quad (1)$$

where $\boldsymbol{M}(\boldsymbol{q}) \in \mathfrak{R}^{\mathrm{m}\times\mathrm{m}}$ is the inertial matrix of rigid link, $\boldsymbol{C}(\boldsymbol{q},\dot{\boldsymbol{q}})\dot{\boldsymbol{q}} \in \mathfrak{R}^{\mathrm{m}\times\mathrm{m}}$ is the Coriolis and centrifugal force vector. $\boldsymbol{\tau} \in \mathfrak{R}^{\mathrm{m}}$ is the applied joint wrench exerted by the cables. $\boldsymbol{J}(\boldsymbol{q}) \in \mathfrak{R}^{\mathrm{m}\times\mathrm{m}}$ is a Jacob matrix and f is the interaction force vector between the robot and the environment such as human body.

In order to control the cable-driven robot, it is necessary to specify the mathematic relationship between the cable tension and wrench acting at the end-effector/joints of the robot, which can be represented as

$$\boldsymbol{AT} = \boldsymbol{\tau} \quad (2)$$

where $\boldsymbol{T} \in \mathfrak{R}^{\mathrm{n}}$ is the cable tension vector of n-dimension satisfying the inequality

$$\boldsymbol{T}_{\boldsymbol{min}} \leq \boldsymbol{T} \leq \boldsymbol{T}_{\boldsymbol{max}} \quad (3)$$

$\boldsymbol{T}_{\boldsymbol{max}} = (\boldsymbol{T}_{\boldsymbol{max1}}, \cdots, \boldsymbol{T}_{\boldsymbol{maxn}})^{\boldsymbol{T}} \in \mathfrak{R}^{\mathrm{n}}$ is the maximum toleration of the cable and is related to the material of the cable, $\boldsymbol{T}_{\boldsymbol{min}} = (\boldsymbol{T}_{\boldsymbol{min1}}, \cdots, \boldsymbol{T}_{\boldsymbol{minn}})^{\boldsymbol{T}} \in \mathfrak{R}^{\mathrm{n}}$ denotes the minimum limitation of the tension which is nonnegative, regularly. $\boldsymbol{\tau}$ represents the wrench vector (torque/force). $\boldsymbol{A} \in \mathfrak{R}^{\mathrm{m}\times\mathrm{n}}$ represents the structure matrix which can be calculated as

$$\boldsymbol{A} = \begin{pmatrix} -\boldsymbol{l_1} & \cdots & -\boldsymbol{l_n} \\ -\boldsymbol{w_1} \times \boldsymbol{l_1} & \cdots & -\boldsymbol{w_n} \times \boldsymbol{l_n} \end{pmatrix},$$

where $\boldsymbol{l_n}$ denotes the tendon vector and $\boldsymbol{w_n}$ represents the center of the platform which is formed by several connection point between the cable and the rigid link (human arm) to each connection point.

Basically, for the given wrench vector $\boldsymbol{\tau} \in \mathfrak{R}^{\mathrm{m}}$, the inverse relation to compute the tension $\boldsymbol{T} \in \mathfrak{R}^{\mathrm{n}}$ with $\boldsymbol{m} < n$ can be calculated as

$$\boldsymbol{T} = \boldsymbol{A}^{+}\boldsymbol{\tau} + (\boldsymbol{I} - \boldsymbol{A}^{+}\boldsymbol{A})\boldsymbol{p} \quad (4)$$

Here $\boldsymbol{A}^{+}$ denotes the pseudo-inverse of $\boldsymbol{A}$, and $(\boldsymbol{I} - \boldsymbol{A}^{+}\boldsymbol{A}) = \boldsymbol{N}(\boldsymbol{A})$ is the orthogonal complement of $\boldsymbol{A}$, and $\boldsymbol{p}$ can be selected as any vector, $\boldsymbol{I}$ is a unit matrix.

Due to the input constraint of the tension of Eq. (3), from Eq. (2), wrench will also have a limitation. The relation between tension constraint and wrench constraint is shown in Fig. 1 with the simple setting that tension space has 2-dimensions and wrench has 1-dimension.

Note that, the angular $\boldsymbol{\varphi}$ between two spaces is totally dependent on the matrix $\boldsymbol{A}$. As shown in Fig. 1 that for a given wrench $\boldsymbol{\tau_\gamma}$, there exist plenty of tension choices to execute due to the multi-selection of $\boldsymbol{p}$ in Eq. (4). Hence, a lot of work has been contributed to the optimization of tension distribution to ensure all tension has been located into the constraint box constructed by tension's limitation. Meanwhile, for a given tension constraint and a given pose (structure matrix $\boldsymbol{A}$), wrench $\boldsymbol{\tau}$ can be denoted as the feasible wrench satisfies the range $\boldsymbol{\tau} \in [\boldsymbol{\tau}_{\boldsymbol{min}}, \boldsymbol{\tau}_{\boldsymbol{max}}]$. However, this range of the wrench may limit the objective task of the robot. For example, if there is a large error between the robot's initial position and its objective target, when using usual PD control, we may not be possible to generate a necessary large wrench $\boldsymbol{\tau}$ outside the constraint range $\boldsymbol{\tau} \in [\boldsymbol{\tau}_{\boldsymbol{min}}, \boldsymbol{\tau}_{\boldsymbol{max}}]$.

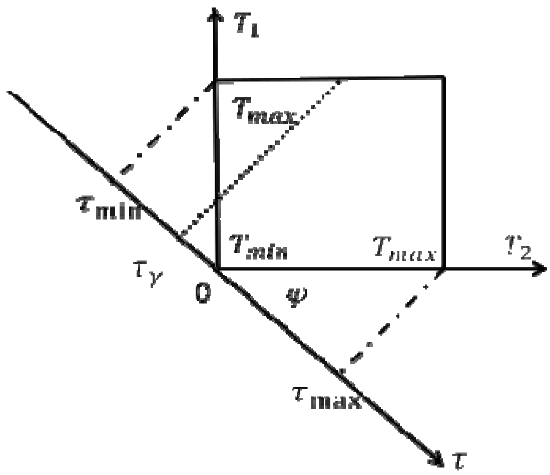

Fig. 1 Relationship between the tension space and torque space.

2.2 Previous Works

First of all, considering the redundant actuation problem that $\boldsymbol{m} < n$, in some previous researches [6], LP as well as QP programming has been used to solve the limitation problem of the tension. This idea can be formulated as following:

$$\begin{aligned} &min\,\boldsymbol{f}(\boldsymbol{p}) \\ &s.t.\boldsymbol{T_{min}} \le \boldsymbol{A}^{+}\boldsymbol{\tau} + (\boldsymbol{I} - \boldsymbol{A}^{+}\boldsymbol{A})\boldsymbol{p} \le \boldsymbol{T_{max}} \end{aligned} \tag{5}$$

If the objective function is selected as $\boldsymbol{f}(\boldsymbol{p}) = \boldsymbol{c^T p}$ ($\boldsymbol{c}$ is a constant vector), it is an LP problem. If $\boldsymbol{f}(\boldsymbol{p}) = \boldsymbol{p^T Y p}$ ($\boldsymbol{Y}$ is a positive definite matrix), it is a QP problem.

However, no matter what the objective function is chosen as and how the vector $\boldsymbol{p}$ varies, there may exist some infeasible $\boldsymbol{\tau}$ that makes unsatisfactory tension's condition. Moreover, since we need iterative computation to solve LP or QP objective functions subjected to some conditions with inequalities, it may be difficult to perform within real time control of the robot.

Secondly, considering the tension limitation problem, in order to keep the cables to satisfy the tension constraint while the robot is executing some tasks, it is necessary to consider the term composing control input $\boldsymbol{\tau}$ (wrench). For tracking task, we cannot set the desired position too far to make the designed wrench too large for robot to handle it. Hence, tracking the desired position outside the tolerance scope is necessary to be considered.

Oh and Agrawal [9] proposed a method to solve this problem for a 6 DOF cable-driven parallel robot with 6 cables. The robot's dynamics in the task space can be determined as

$$\boldsymbol{M}(\boldsymbol{X})\ddot{\boldsymbol{X}} + \boldsymbol{C}(\boldsymbol{X},\dot{\boldsymbol{X}})\dot{\boldsymbol{X}} + \boldsymbol{g}(\boldsymbol{X}) = \boldsymbol{AT} \tag{6}$$

where $\boldsymbol{X} = (\boldsymbol{x},\boldsymbol{y},\boldsymbol{z},\boldsymbol{\psi},\boldsymbol{\theta},\boldsymbol{\phi})$ describes the position and orientation of the end-effector, $\boldsymbol{g}(\boldsymbol{X})$ represents the gravity vector. Note that, since we have $m = n = 6$ here, the matrix $\boldsymbol{A}$ is invertible.

They first set the control input tension vector $\boldsymbol{T}$ as

$$\begin{aligned} \boldsymbol{T} = \boldsymbol{A}^{-1}(\boldsymbol{C}(\boldsymbol{X},\dot{\boldsymbol{X}})\dot{\boldsymbol{X}} + \boldsymbol{g}(\boldsymbol{X}) - \boldsymbol{M}(\boldsymbol{X})\boldsymbol{\lambda}\dot{\boldsymbol{X}} \\ - \boldsymbol{M}(\boldsymbol{X})\boldsymbol{\eta s}) \end{aligned} \tag{7}$$

where $\lambda = \lambda_0 \boldsymbol{I}$, $\eta = \eta_0 \boldsymbol{I}$, $\boldsymbol{s}$ is the control surface defined by

$$\boldsymbol{s} = \dot{\boldsymbol{X}} + \boldsymbol{\lambda}(\boldsymbol{X} - \boldsymbol{X_d}) \tag{8}$$

By imposing a relation that $\dot{\boldsymbol{s}} = -\boldsymbol{\eta s}$, the equilibrium at the $\boldsymbol{X_d}$ will be exponentially stable and we have

$$\ddot{\boldsymbol{X}} = -\boldsymbol{\lambda}\dot{\boldsymbol{X}} - \boldsymbol{\eta s} \tag{9}$$

Let the $\boldsymbol{X_d}$ be the input, considering the first term of the robot's position vector $\boldsymbol{X}$, the transfer function can be written as

$$x(r) = \frac{\eta_0\lambda_0}{r^2 + (\lambda_0 + \eta_0)r + \eta_0\lambda_0} x_d(r) \tag{10}$$

After some analyses of the transfer function, it is possible to obtain the damping ratio $\boldsymbol{\zeta} \ge \boldsymbol{1}$ and the natural frequency $\boldsymbol{\omega_n} = \sqrt{\boldsymbol{\eta_0\lambda_0}}$.

Then, based on the analysis of time domain solution of the transfer function, we can get the bounds on states:

$$x(t) \in [x_0, x_d]$$
$$\ddot{x}(t) \in (x_0 - x_d){\omega_n}^2[Z_m, -1]$$

where $\boldsymbol{x_0}$ is the initial value of the position and $\boldsymbol{Z_m}$ represents the maximum of the term

$$\frac{1}{2\sqrt{\zeta^2 - 1}}[-\left(\zeta + \sqrt{\zeta^2 - 1}\right)e^{-\left(\zeta + \sqrt{\zeta^2-1}\right)\omega_n t} + (\zeta + \sqrt{\zeta^2 - 1})e^{\left(-\zeta + \sqrt{\zeta^2 - 1}\right)\omega_n t}] \tag{11}$$

Thus, we can compute the bounds on other components of vector x and $\ddot{x}$.

Then, this research considered the translation motion of the robot and simplified the tension constraint as

$$\boldsymbol{T} = \boldsymbol{A}^{-1}(\boldsymbol{M}(\boldsymbol{x})\ddot{\boldsymbol{x}} + \boldsymbol{g}(\boldsymbol{x})) \ge \boldsymbol{0} \tag{12}$$

This inequality is determined by $\mathbf{x}$, $\ddot{\mathbf{x}}$ and some coefficients. In order to make this inequality satisfied, it is necessary to calculate the minimum value of $\boldsymbol{T}$ by substituting the bounds of $\boldsymbol{x}$, $\ddot{\boldsymbol{x}}$ into this inequality. Note that when the coefficient in front of the variable is minus, we need to substitute the maximum value of this valuable and when the coefficient is positive, we should substitute the minimum value. After substituting, we can get

$$\boldsymbol{D_1}\begin{bmatrix}x_d\\ y_d\end{bmatrix} \le \boldsymbol{D_2}\begin{bmatrix}x_0\\ y_0\end{bmatrix} + \boldsymbol{b} \quad (13)$$

Note that, this research simplified the problem as robot only moves in the x-y plane. Matrix $\boldsymbol{D_1}\,\boldsymbol{D_2}$ and vector $\boldsymbol{b}$ can be calculated by the bounds of each components in $\boldsymbol{X}$ and $\ddot{\boldsymbol{X}}$. Thus, Eq. (13) determines a feasible domain of $\boldsymbol{X_d}$ based on the initial position.

In order to track the final objective position, it is necessary to select the closest one in the feasible domain of $\boldsymbol{x_d}$ to the final objective position. In the research of Ref. [9], they further offered an iteration optimization method to perform the iteration calculation with the movement of the robot and chose the most appropriate desired position in the calculated scope, which is closest to the final desired position.

Although this work shows some efficiency on the position control task, it is impossible to be used for the trajectory tracking control problem of cable-driven robot, especially with high dimensional redundant tension due to the massive computation time and its complicate analysis.

As mentioned in the previous analysis, the cable's tension constraint condition as well as its actuation redundancy are two fundamental problems that we should consider in the control design of the cable-driven robot. If we do not design the proper control, these two problems may constrain the possible selection of the robot's objective target position for some given initial positions so as to seriously limit the robot's task performance. By now, the researches mainly considered only one side of the problems, static solution of the redundancy or dynamic control under tension limitations. In order to make real application of a cable driven robot to perform wider range of tasks, we need to solve the two problems simultaneously for the dynamics of the robot.

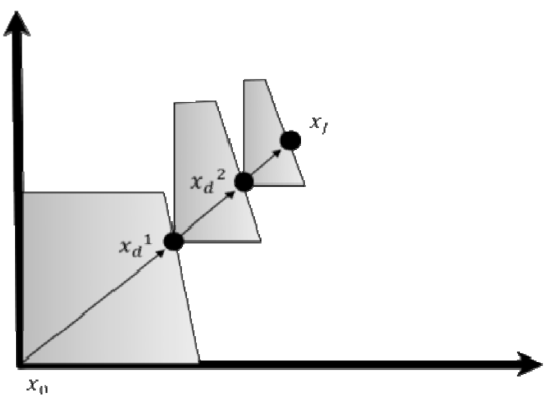

Fig. 2 Reachable domains in an x-y plane.

3. Dynamic Control of Cable-Driven Robot Using PVFC

In order to solve the redundancy problem as well as the tension limitation problem so as the robot can realize more dynamic task performance under cable-driven actuation, in this paper, we propose a novel dynamic control approach. Here, we specify the robot's objective motions in a form of the velocity vector field in the work space instead of the usual time function. We then set an augmented virtual dynamic subsystem with dimension *n*-*m*. For the *n*-dimensional augmented dynamic system, we apply Li's PVFC [10] to design the control input. PVFC can realize not only the motion tracking performance for the real robot's velocity to approach the objective velocity field vector in free motion space but also the passivity when the robot is interacting with the environment. Finally, to keep the real robot's cable tension limitation, we adjust the PVFC's control parameter and clarify the control parameter's possible range.

3.1 Tracking of the Desired Velocity Vector Field

In the position feedback control of a cable driven robot, as we analyzed in Section 2, it is difficult to plan the desired position $\boldsymbol{X_d}$ $(\boldsymbol{t})$ for some initial position $\boldsymbol{X_0}$ $(\boldsymbol{t})$ considering the cable tension's limitation.

In this paper, in order to trace the trajectory, we formulate the objective motion of the robot as a velocity vector field $\boldsymbol{V}(\boldsymbol{q})$ (time invariant) with

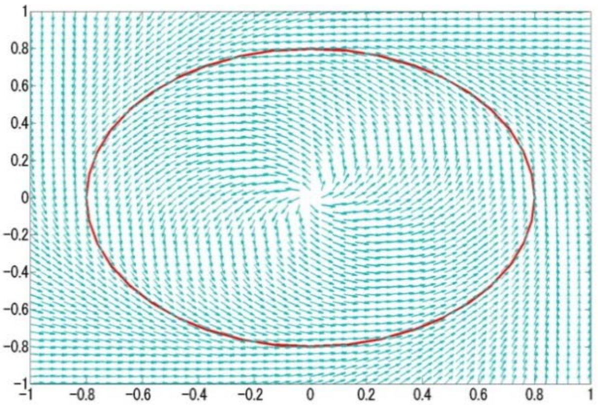

Fig. 3 Position based desired velocity field.

respect to the robot's position vector q. As shown in Li's work [10], if $\mathbf{q} \in \mathscr{g}$ (a m-dimension configuration manifold), then we can denote the tangent space of $\mathscr{g}$ as $\mathbf{T_q}\mathscr{g}$ at one q and desired velocity field V is a map $\mathbf{V}: \mathscr{g} \to \mathbf{T}\mathscr{g}$; $\mathbf{q} \to \mathbf{V}(\mathbf{q})$ where $\mathbf{T}\mathscr{g} = \bigcup_{q \in \mathscr{g}} \boldsymbol{T_q}\mathscr{g}$, $\mathbf{T}\mathscr{g}$ is the tangent bundle of the manifold $\mathscr{g}$.

Notice that, design of V(q) constructs a desired velocity vector at each point in the workspace so as to replace the task of tracking the final trajectory by the tracing of the desired vector at each point.

In order to build the map V(q), firstly, we construct a potential function $\boldsymbol{P_o}(\boldsymbol{q})$ with respect to $\boldsymbol{q}$ and this function is required to have the maximum value at the desired trajectory leading $\boldsymbol{P_o}(\boldsymbol{q})$'s gradient can have the minimum size zero at the desired trajectory and can represent the normal vectors of the desired trajectory. Therefore, gradient of $\boldsymbol{P_o}(\boldsymbol{q})$ can be used as one part of V. On the another side, we can also design a perpendicular vector of this gradient as the tangential vector of the desired trajectory which is required to have smaller size at points away from desired trajectory and have maximum size at the desired trajectory. Both normal and tangential desired vector constitute a desired velocity vector V at each point.

3.2 Augmented Mechanical System

In order to overcome the difficulty brought by the redundancy characteristic of the robot's cable actuation of Eqs. (1) and (2) with $m < n$, we propose to augment the system with a *n-m* dimensional virtual dynamic subsystem.

$$\boldsymbol{M_F}\ddot{\boldsymbol{q}}_{n-m} = \boldsymbol{\tau}_{n-m} = \boldsymbol{BT} \tag{14}$$

where we set $\boldsymbol{M_F} = \mathbf{diag}(\boldsymbol{m_f}, \cdots, \boldsymbol{m_f}) \in \Re^{(\boldsymbol{n}-\boldsymbol{m})\times(\boldsymbol{n}-\boldsymbol{m})}$ and $\boldsymbol{B}$ represents a $(\boldsymbol{n}-\boldsymbol{m}) \times \boldsymbol{n}$ matrix, $\boldsymbol{q_{n-m}} \in \Re^{(\boldsymbol{n}-\boldsymbol{m})}$ is the position vector of the virtual augmented subsystem.

Therefore, the dynamic of the overall augmented system can be formulated as

$$\overline{\boldsymbol{M}}(\overline{\boldsymbol{q}})\ddot{\overline{\boldsymbol{q}}} + \overline{\boldsymbol{C}}(\overline{\boldsymbol{q}}, \dot{\overline{\boldsymbol{q}}})\dot{\overline{\boldsymbol{q}}} = \overline{\boldsymbol{\tau}} + \overline{\boldsymbol{\tau}}_{\boldsymbol{e}} \tag{15}$$

where

$$\overline{\boldsymbol{M}}(\overline{\boldsymbol{q}}) = \begin{bmatrix} \boldsymbol{M}(\boldsymbol{q}) & \mathbf{0} \\ \mathbf{0} & \boldsymbol{M_F} \end{bmatrix},$$

$$\overline{\boldsymbol{C}}(\overline{\boldsymbol{q}}, \dot{\overline{\boldsymbol{q}}}) = \begin{bmatrix} \boldsymbol{C}(\boldsymbol{q}, \dot{\boldsymbol{q}}) & \mathbf{0} \\ \mathbf{0} & \mathbf{0} \end{bmatrix},$$

$$\overline{\boldsymbol{q}} = \begin{bmatrix} \boldsymbol{q} \\ \boldsymbol{q_{n-m}} \end{bmatrix},$$

$$\overline{\boldsymbol{\tau}}_{\boldsymbol{e}} = \begin{bmatrix} \boldsymbol{\tau_e} \\ \mathbf{0} \end{bmatrix}$$

In detail, $\overline{\boldsymbol{q}} = [\boldsymbol{q_1}, \cdots, \boldsymbol{q_m}, \boldsymbol{q_{m+1}}, \cdots, \boldsymbol{q_n}]^{\boldsymbol{T}}$, and by combining Eqs. (2) and (15), we have

$$\overline{\boldsymbol{\tau}} = \overline{\boldsymbol{A}}\boldsymbol{T} = \begin{pmatrix} \boldsymbol{A} \\ \boldsymbol{B} \end{pmatrix}\boldsymbol{T} \tag{16}$$

Notice that, in order to avoid appearance of redundancy, we should select the matrix *B* so that to keep the augmented matrix $\begin{pmatrix} \boldsymbol{A} \\ \boldsymbol{B} \end{pmatrix}$ full rank.

The objective velocity vector $\boldsymbol{V_{n-m}}(\boldsymbol{q})$ for the augmented subsystem can be specified as follows.

Firstly, we define

$$\overline{\boldsymbol{V}}(\overline{\boldsymbol{q}}) = [\boldsymbol{V}(\boldsymbol{q})^{\boldsymbol{T}}, \boldsymbol{V_{n-m}}(\boldsymbol{q})]^{\boldsymbol{T}} \tag{17}$$

as the objective velocity vector of the augmented system, then the total objective kinetic energy can be denoted as

$$k(\overline{\boldsymbol{q}}, \overline{\boldsymbol{V}}(\overline{\boldsymbol{q}})) = \frac{\mathbf{1}}{\mathbf{2}}\overline{\boldsymbol{V}^{\boldsymbol{T}}}(\overline{\boldsymbol{q}})\overline{\boldsymbol{M}}(\overline{\boldsymbol{q}})\overline{\boldsymbol{V}}(\overline{\boldsymbol{q}})$$

$$= \frac{\mathbf{1}}{\mathbf{2}}(\boldsymbol{V^T}\boldsymbol{M}(\boldsymbol{q})\boldsymbol{V} + \boldsymbol{V_{n-m}}^{\boldsymbol{T}}\boldsymbol{M_F}\boldsymbol{V_{n-m}}) = \bar{E} > 0 \tag{18}$$

where $\boldsymbol{V_{n-m}} = \boldsymbol{\rho}[\mathbf{1}, \cdots, \mathbf{1}]^{\boldsymbol{T}}$ and $\boldsymbol{\rho}$ are a scalar. For the given $\boldsymbol{V}(\boldsymbol{q})$ and constant $\overline{\boldsymbol{E}}$, we then can calculate

$$\rho = \sqrt{\frac{2}{\boldsymbol{m_f}}\left(\bar{E} - \frac{1}{2}\boldsymbol{V^T M}(\boldsymbol{q})\boldsymbol{V}\right)} \tag{19}$$

Then, based on $\boldsymbol{\rho}$, it is possible to calculate the virtual subsystem's desired velocity $\boldsymbol{V_{n-m}}$ and further the desired velocity of total augmented system $\overline{\boldsymbol{V}}$.

3.3 Coupling Control Law

Before considering the cable tension limitation problem, for the control design of the augmented system such that the original cable robot system can realize not only the tracking of the objective velocity vector $\overline{\boldsymbol{V}}$ in the free motion space (when $\boldsymbol{\tau_e}= 0$) but also be passive when interacting with environment, we simply apply LI's PVFC control rule. From Ref. [10], we can set a control input as

$$\bar{\boldsymbol{\tau}}(\bar{\boldsymbol{q}}, \dot{\bar{\boldsymbol{q}}}) = \boldsymbol{G}\dot{\bar{\boldsymbol{q}}} + \gamma\boldsymbol{R}\dot{\bar{\boldsymbol{q}}} = \bar{\boldsymbol{\tau}}_c(\bar{\boldsymbol{q}}, \dot{\bar{\boldsymbol{q}}}) + \overline{\boldsymbol{\tau}_f}(\bar{\boldsymbol{q}}, \dot{\bar{\boldsymbol{q}}}) \tag{20}$$

defining $\boldsymbol{G}$ and $\boldsymbol{R}$ as two skew symmetric matrices

$$\boldsymbol{G} = \frac{\boldsymbol{1}}{2\overline{\boldsymbol{E}}}(\bar{\boldsymbol{w}}\overline{\boldsymbol{P}}^{\boldsymbol{T}} - \overline{\boldsymbol{P}}\bar{\boldsymbol{w}}^{\boldsymbol{T}}) \tag{21}$$

$$\boldsymbol{R} = (\overline{\boldsymbol{P}}\bar{\boldsymbol{p}}^{\boldsymbol{T}} - \bar{\boldsymbol{p}}\overline{\boldsymbol{P}}^{\boldsymbol{T}}) \tag{22}$$

where

$$\bar{\boldsymbol{p}}(\bar{\boldsymbol{q}}, \dot{\bar{\boldsymbol{q}}}) = \overline{\boldsymbol{M}}(\bar{\boldsymbol{q}})\dot{\bar{\boldsymbol{q}}}$$

$$\overline{\boldsymbol{P}}(\bar{\boldsymbol{q}}) = \overline{\boldsymbol{M}}(\bar{\boldsymbol{q}})\overline{\boldsymbol{V}}(\bar{\boldsymbol{q}})$$

$$\bar{\boldsymbol{w}}(\bar{\boldsymbol{q}}, \dot{\bar{\boldsymbol{q}}}) = \overline{\boldsymbol{M}}(\bar{\boldsymbol{q}})\dot{\overline{\boldsymbol{V}}}(\bar{\boldsymbol{q}}) + \overline{\boldsymbol{C}}(\bar{\boldsymbol{q}}, \dot{\bar{\boldsymbol{q}}})\overline{\boldsymbol{V}}(\bar{\boldsymbol{q}})$$

This control input leads to two results:

The trajectory tracking error of the total augmented robot system ($\overline{\boldsymbol{e_a}} = \dot{\bar{\boldsymbol{q}}} - \boldsymbol{\beta}\overline{\boldsymbol{V}}$) can be globally exponentially stable which also makes the original system exponentially convergent to the desired trajectory.

System can be passive when there are external forces acting at the system.

The proof of these two results can refer to Ref. [10].

3.4 Satisfaction of the Tension Condition

3.4.1 Analysis of the Tension's Condition

The important thing left here is to adjust $\bar{\boldsymbol{\tau}}$ of Eq. (20) to satisfy the tension condition $(\boldsymbol{T_{min}} \leq \boldsymbol{T} \leq \boldsymbol{T_{max}})$ which can be also represented as

$$(\boldsymbol{T} - \boldsymbol{T_0})^{\boldsymbol{T}}\boldsymbol{E}(\boldsymbol{T} - \boldsymbol{T_0}) \leq \boldsymbol{1} \tag{23}$$

where

$$\boldsymbol{T_0} = \frac{\boldsymbol{T_{max}} + \boldsymbol{T_{min}}}{\boldsymbol{2}}$$

$$\boldsymbol{E} = \boldsymbol{diag}(\frac{\boldsymbol{1}}{\boldsymbol{r^2}}, \cdots, \frac{\boldsymbol{1}}{\boldsymbol{r^2}})$$

and

$$\boldsymbol{r} = \frac{\boldsymbol{max}\,(\boldsymbol{T_{maxi}}) - \boldsymbol{min}\,(\boldsymbol{T_{minj}})}{\boldsymbol{2}}$$

From Eq. (2), since we select B so that $\overline{\mathbf{A}} = \binom{\mathbf{A}}{\mathbf{B}}$ is full rank, we have

$$\boldsymbol{T} = \overline{\boldsymbol{A}}^{-\boldsymbol{1}}\bar{\boldsymbol{\tau}} \tag{24}$$

For $\mathbf{T_0}$, there exists an corresponding $\bar{\boldsymbol{\tau}}_{\mathbf{0}}$ that

$$\bar{\boldsymbol{\tau}}_{\boldsymbol{0}} = \overline{\boldsymbol{A}}\boldsymbol{T_0} \tag{25}$$

Then, the cycle constraint Eq. (23) can be represented as

$$\left(\overline{\boldsymbol{A}}^{-\boldsymbol{1}}\left(\boldsymbol{G}\dot{\bar{\boldsymbol{q}}} + \gamma\boldsymbol{R}\dot{\bar{\boldsymbol{q}}}\right) - \boldsymbol{T_0}\right)^{\boldsymbol{T}}\left(\overline{\boldsymbol{A}}^{-\boldsymbol{1}}\left(\boldsymbol{G}\dot{\bar{\boldsymbol{q}}} + \gamma\boldsymbol{R}\dot{\bar{\boldsymbol{q}}}\right) - \boldsymbol{T_0}\right) - r^2 \leq 0 \tag{26}$$

by considering Eq. (21).

From Eq. (26), it is clear that we can change the value of $\boldsymbol{\gamma}$ to make the tension condition be satisfied. Based on this design, we can regard the left side of Eq. (26) as a function with variable $\boldsymbol{\gamma}$

$$f(\gamma) = \gamma^2\boldsymbol{a^T a} - 2\gamma\boldsymbol{a^T b} + \boldsymbol{b^T b} - r^2 = 0 \tag{27}$$

where $\boldsymbol{a} = \overline{\boldsymbol{A}}^{-\boldsymbol{1}}\boldsymbol{R}\dot{\bar{\boldsymbol{q}}}$ and $\boldsymbol{b} = \boldsymbol{T_0} - \overline{\boldsymbol{A}}^{-\boldsymbol{1}}\boldsymbol{G}\dot{\bar{\boldsymbol{q}}}$

If there is no real solution of this function, the adjustable range of $\boldsymbol{\gamma}$ should not exist. Therefore, besides the appropriate adjustment of $\boldsymbol{\gamma}$, we also need to select an appropriate $\overline{\mathbf{A}}$.

3.4.2 Method to Satisfy Tension Condition

In order to satisfy the constraint Eq. (26), we need to minimize the norm of the vector

$$\Delta\boldsymbol{T_c} = (\boldsymbol{T_0} - \overline{\boldsymbol{A}}^{-\boldsymbol{1}}(\boldsymbol{G}\dot{\bar{\boldsymbol{q}}} + \boldsymbol{\gamma}\boldsymbol{R}\dot{\bar{\boldsymbol{q}}}))$$

as possible as we can.

If we select the inverse of the $\overline{\boldsymbol{A}}$ as

$$\overline{\boldsymbol{A}}^{-\boldsymbol{1}} = (\boldsymbol{A}^{+}\ \boldsymbol{N_A}\boldsymbol{K}) \tag{28}$$

where $\boldsymbol{K} = diag(k_1, \cdots, k_{n-m})$ can be selected to satisfy the equation, the vector $\Delta\boldsymbol{T_c}$ can be rewritten as

$$\Delta \boldsymbol{T_c} = \boldsymbol{T_0} - \boldsymbol{A}^{+}(\bar{\boldsymbol{\tau}}_{\boldsymbol{Gm}} + \gamma\bar{\boldsymbol{\tau}}_{\boldsymbol{Rm}}) - \boldsymbol{N_A}\boldsymbol{K}(\bar{\boldsymbol{\tau}}_{\boldsymbol{Gnm}} + \gamma\bar{\boldsymbol{\tau}}_{\boldsymbol{Rnm}}) \quad (29)$$

where $\bar{\boldsymbol{\tau}}_{\boldsymbol{Gm}}$ and $\bar{\boldsymbol{\tau}}_{\boldsymbol{Rm}}$ represent the first $\boldsymbol{m}$ elements of the vector $\boldsymbol{G}\dot{\boldsymbol{q}}$ and $\boldsymbol{R}\dot{\boldsymbol{q}}$, $\bar{\boldsymbol{\tau}}_{\boldsymbol{Gnm}}$ and $\bar{\boldsymbol{\tau}}_{\boldsymbol{Rnm}}$ represent the remaining $\boldsymbol{n}-\boldsymbol{m}$ elements of the $\boldsymbol{G}\dot{\boldsymbol{q}}$ and $\boldsymbol{R}\dot{\boldsymbol{q}}$. $\boldsymbol{N_A}$ represents the null space of the matrix $\boldsymbol{A}$.

Notice that, if we select $\bar{\mathbf{A}}^{-1}$ as Eq. (28), $\bar{\mathbf{A}}$ would satisfy $\bar{\mathbf{A}} = \begin{pmatrix}\mathbf{A}\\ \mathbf{B}\end{pmatrix}$ which is proved in Ref. [11].

Based on Eq. (29), it is easy to know that, when we have a certain $\bar{\boldsymbol{\tau}}$, the norm of $\Delta\boldsymbol{T_c}$ could have the minimum value by appropriately selecting each element of the diagonal matrix $\mathbf{K}$ to make it satisfy

$$\boldsymbol{K}(\bar{\boldsymbol{\tau}}_{\boldsymbol{Gnm}} + \gamma\bar{\boldsymbol{\tau}}_{\boldsymbol{Rnm}}) = \boldsymbol{N_A}^{+}(\boldsymbol{T_0} - \boldsymbol{A}^{+}(\bar{\boldsymbol{\tau}}_{\boldsymbol{Gm}} + \bar{\boldsymbol{\tau}}_{\boldsymbol{Rm}})) \quad (30)$$

Thus, the minimum value of $\Delta\boldsymbol{T_c}$ can be formulated as

$$\Delta\boldsymbol{T_c} = (\boldsymbol{I} - \boldsymbol{N_A}\boldsymbol{N_A}^{+})(\boldsymbol{T_0} - \boldsymbol{A}^{+}(\bar{\boldsymbol{\tau}}_{\boldsymbol{Gm}} + \gamma\bar{\boldsymbol{\tau}}_{\boldsymbol{Rm}})) \quad (31)$$

From this result, Eq. (26) can be written as

$$\|\gamma\boldsymbol{w} - \boldsymbol{v}\| \le r \quad (32)$$

where $\boldsymbol{w} = (\boldsymbol{I} - \boldsymbol{N_A}\boldsymbol{N_A}^{+})\boldsymbol{A}^{+}\bar{\boldsymbol{\tau}}_{\boldsymbol{Rm}}$

$\boldsymbol{v} = (\boldsymbol{I} - \boldsymbol{N_A}\boldsymbol{N_A}^{+})(\boldsymbol{T_0} - \boldsymbol{A}^{+}\bar{\boldsymbol{\tau}}_{\boldsymbol{Gm}})$.

From the result of reverse triangular inequality, we can get

$$r \ge \|\gamma\boldsymbol{w} - \boldsymbol{v}\| \ge |\gamma\|\boldsymbol{w}\| - \|\boldsymbol{v}\|| \quad (33)$$

Thus, after some algebra analysis, we obtain the condition for the control parameter γ as

$$\frac{\|\boldsymbol{v}\| - r}{\|\boldsymbol{w}\|} \le \gamma \le \frac{r + \|\boldsymbol{v}\|}{\|\boldsymbol{w}\|} \quad (34)$$

Consequently, we can solve the tension's problem following two steps:

(1) Select γ satisfying Eq. (34).

(2) Select the inverse of $\bar{\boldsymbol{A}}$ as Eqs. (28)-(30).

Thus, we can overcome the problem brought by the limitation of cable tension so as to control the cable-driven robot tracking trajectory while keeping the passivity contemporarily.

4. Simulation Result

We performed simulations to verify the effectiveness of our method for a 2-DOF robot driven by 6 cables shown in Fig. 4 tracking a desired trajectory in the x-y plane. The robot's physical parameters used for simulation are listed in Table 1, where I_1 and I_2 represent the inertial moment of each link's center of gravity, m_1 and m_2 represent mass of link, and L_1 and L_2 represent the length of each link.

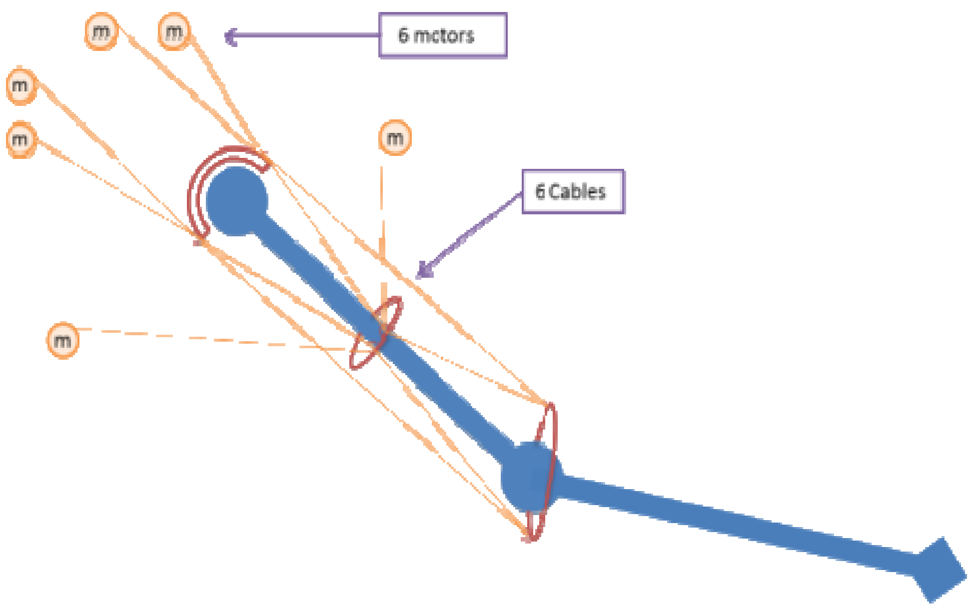

Fig. 4 A 2-link cable driven manipulator.

Table 1 Physical parameter of the robot arm.

I_1	0.625	kgm^2
I_2	0.625	kgm^2
m_1	1	kg
m_2	1	kg
L_1	1	m
L_2	1	m

4.1 Design of Desired Velocity Field

There exist many kinds of choices of potential function $P_o(q)$ to determine the velocity field. In this simulation, we set potential function as a Gaussian Function $P(q) = \exp\left(-\frac{d^2}{\sigma^2}\right)$ such that the gradient of $P(q)$ would have the minimum size zero at the desired trajectory (shown in Fig. 5a), where $d \equiv \left|\sqrt{(x(q)-x0)^2+(y(q)-y0)^2}-R\right|$ and σ is a scalar to determine the Gaussian RMS (root mean square)'s width. R and (x0, y0) represent the radius and the centre point of the desired circle respectively.

Hence, we can calculate the normal vector V^n of the desired trajectory as

$$V^n = grad\ P_o(q) = gradP(x_r, y_r)$$
$$= \frac{-2d}{\sigma^2} exp\left(-\frac{d^2}{\sigma^2}\right)(v_{n1}, v_{n2})^T$$

where

$$v_{n1} = \frac{(x-x0)}{\sqrt{(x-x0)^2+(y-y0)^2}}$$

$$v_{n2} = \frac{(y-y0)}{\sqrt{(x-x0)^2+(y-y0)^2}}$$

The tangential vector of the desired trajectory which is perpendicular to the normal vector can be calculated as

$$V^t = exp\left(-\frac{d^2}{\sigma^2}\right)(v_{n2}, -v_{n1})^T$$

The desired velocity vector at each point can be calculated as

$$V = V^n + V^t$$

The desired trajectory is set as a circle (shown in Fig. 5a) with centre point [0.8, 0.8] and radius r = 0.5.

4.2 Trajectory Tracking Ability

Figs. 5 and 6 show the position tracking results of the cable-driven robot while the control input tension T has been designed following Eq. (24). Fig. 5 shows the desired velocity field of a circle trajectory with centre point (0.8, 0.8) and radius 0.5. In Figs. 6a and 6b, γ is selected as $\gamma = 1$ and $\gamma = 5$ respectively, it is obvious that both selections have a good property of tracking the desired trajectory.

4.3 Satisfaction of Tension's Condition

In these two selections of γ, $\gamma = 1$ can satisfy Eq. (36) while $\gamma = 5$ is disable to satisfy this

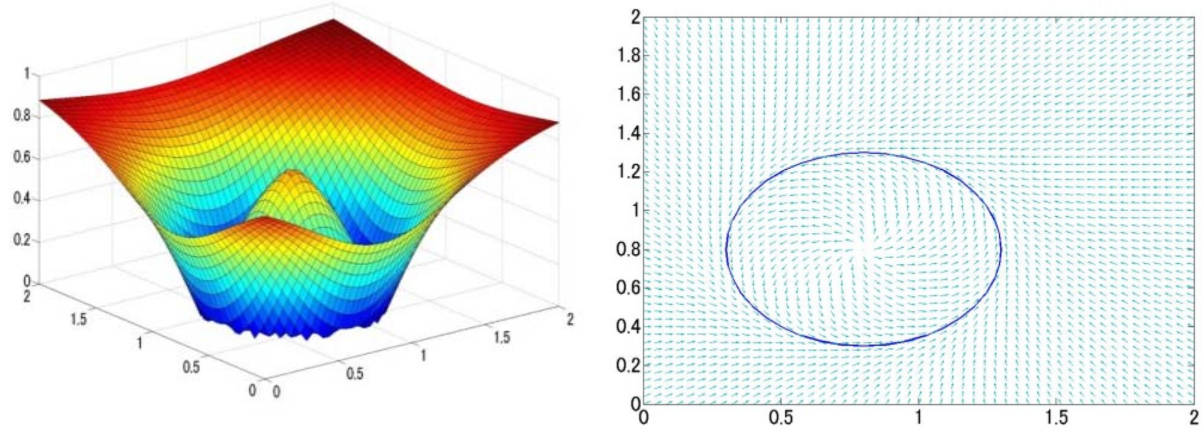

(a) Size of the gradient of $\exp\left(-\frac{d^2}{\sigma^2}\right)$ (b) Velocity field of the desired circle

Fig. 5 Design of the velocity field.

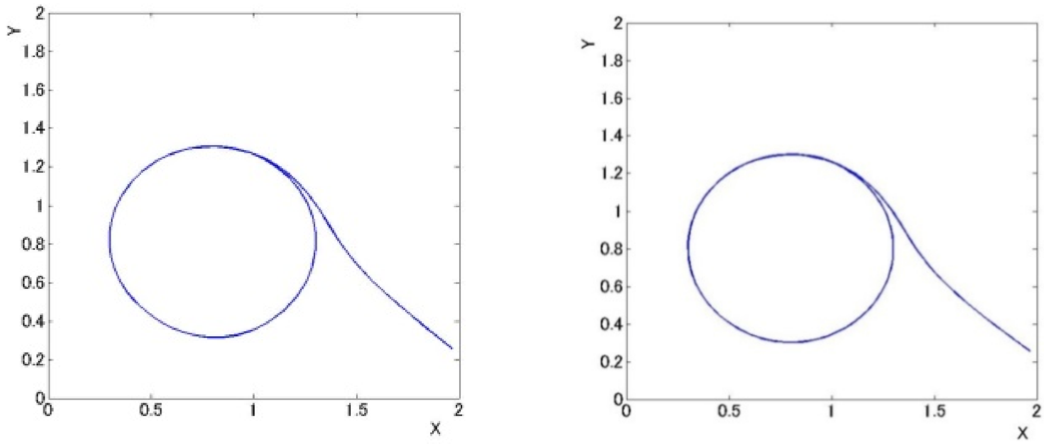

$\gamma = 1$ $\gamma = 5$

Fig. 6 Trajectory of the manipulator's end-effector.

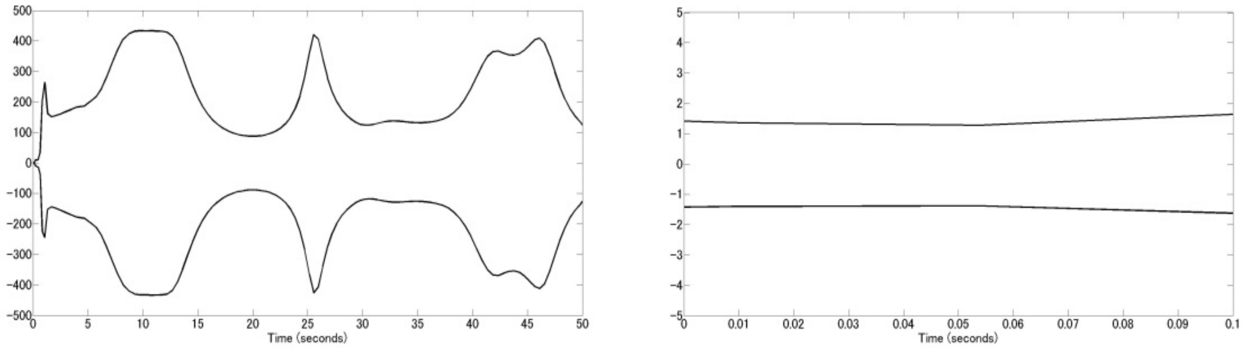

Total upper and lower bound Upper and lower bound at the initial time

Fig. 7 Upper and lower bound of the γ when γ is selected as $\gamma = 1$.

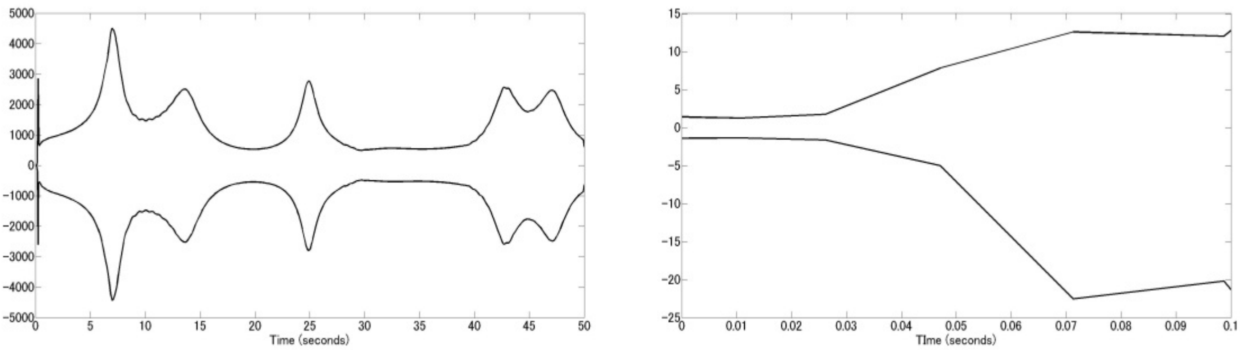

Total upper and lower bound Upper and lower bound at the initial time

Fig. 8 Upper and lower bound of the γ when γ is selected as $\gamma = 5$.

condition. We can check Figs. 7 and 8 representing upper and lower bound in Eq. (36) while using each γ.

From Figs. 7 and 8, it is clear that the selection of γ=1 satisfies the condition in Eq. (36) in total trajectory tracking's procedure while the selection of $\gamma = 5$ is not in the γ's selectable range at the initial time.

Figs. 9 and 10 show the cable tension's result while robot is tracking the desired circle with different selection of γ in control input (Eq. (24)). The upper and lower bound of the tension value is set as 0 N and 5 N.

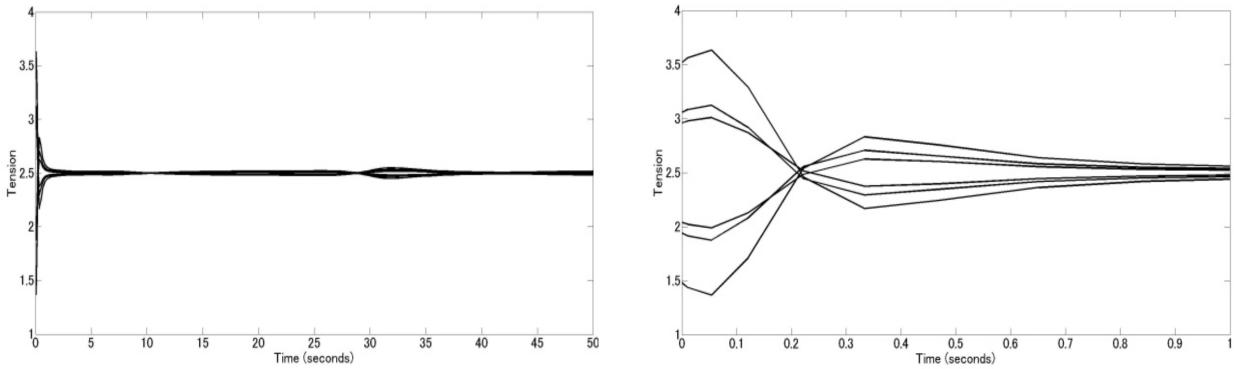

Tension's result of total motion Tension's result of the initial time

Fig. 9 Value of the cable's tension when γ is selected as $\gamma = 1$.

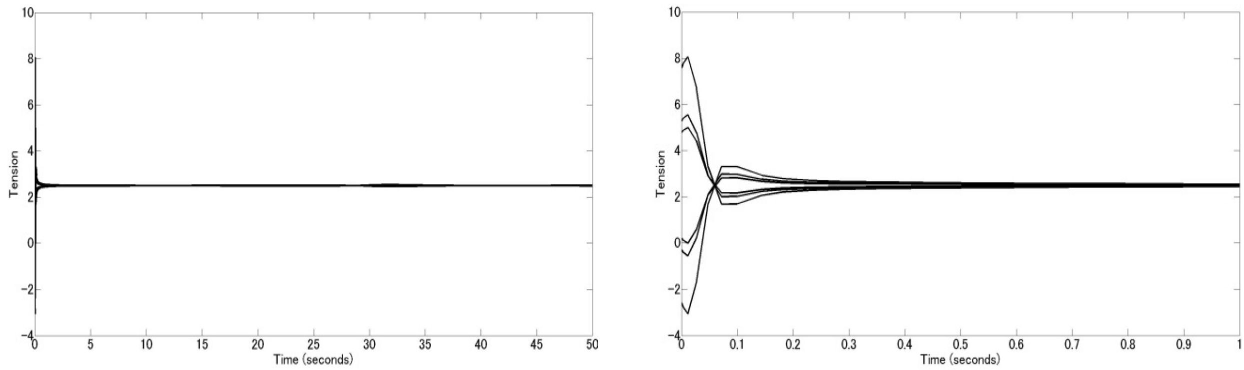

Tension's result of total motion Tension's result of the initial time

Fig. 10 The value of the cable tension ($\gamma = 5$).

From Fig. 9, it is clear that when γ is properly selected, the cable tension may satisfy the tension constraint using our method. From Fig. 10, we see that, if γ is out of the range proposed in Eq. (36), the cable tension may not satisfy the constraint and cables cannot generate such a PVFC's control torque in Eq. (24) at manipulator's joint.

4.4 Passivity of Total Robot System

In x-y plane, we set a stiff wall at the line $x + y = 1$ with a stiffness ratio $ke = 100$ and damper ratio $de = 20$ to test robot's passivity after punching the wall. We select appropriate $\gamma = 1$ in the control torque. The trajectory tracking's result can be shown as below.

From Fig. 11, we see that cable-driven manipulator performs well in trajectory tracking task while interacting with the environment. Meanwhile, from Fig. 12, cables' tension does not violate the constraint in this procedure. From Fig. 13, it is clear that the whole system's kinetic energy would not exceed its initial value after punching the wall, which means that the passivity of the manipulator is satisfied.

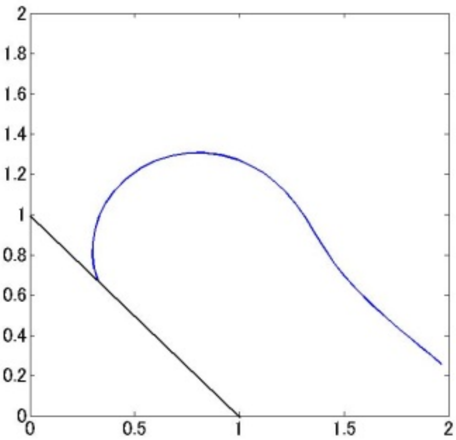

Fig. 11 Trajectory of the manipulator interacting with a stiff wall .

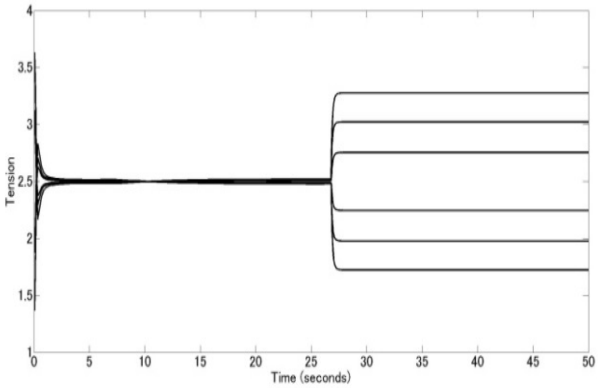

Fig. 12 Cable's tension when robot interacting with a stiff wall.

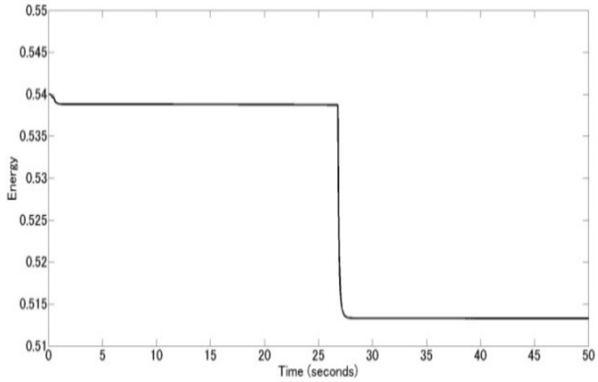

Fig. 13 Total kinetic energy of the whole system.

5. Conclusions

In this research, we studied the dynamic control of a cable driven robot with the cable's tension limitation as well as the cable's redundancy in order to complete the passive trajectory tracking control while keeping the passivity. We first augmented a virtual subsystem to eliminate the redundancy of the original system so that we can easily transfer the tension constraint condition into the wrench space. Then, we use PVFC control method to handle the convergence task of the trajectory tracking and the satisfaction of passivity. After analyzing this PVFC's control input in the wrench space, we derived a condition to adjust the control parameter so as to solve the cable's tension limitation. Compared with other previous researches, this method enables the trajectory tracking control of the cable-driven robot with an easy wrench adjustment algorithm and no heavy optimization for tension distribution.

We also performed simulations to verify the effectiveness of this research. The comparison results showed that robot driven by cables can track the trajectory while keeping its passivity at the same time very well.

Acknowledgement

This research has been partially supported by National Natural Science Foundation of China under Grant No. 61472117.

References

[1] Alp, A. B., and Agrawal, S. K. 2002. "Cable Suspended Robots: Design, Planning and Control." In *Proceedings of the 2002 IEEE International Conference on Robotics and Automation,* Washington, D.C., 4275-80.

[2] Pham, C. B., Yeo, S. H., YANG, G., Kurbanhusen, M. S., and CHEN, I. M. 2006. "Force-Closure Workspace Analysis of Cable-Driven Parallel Mechanisms." *Mechanism and Machine Theory* 41 (1): 53-69.

[3] Mustafa, S. K., and Agrawal, S. K. 2012. "On the Force-Closure Analysis of N-DOF Cable-Driven Open Chains Based on Reciprocal Screw Theory." *IEEE Transactions on Robotics* 28 (1): 22-31.

[4] Duan, Q. J., Vashista, V., and Agrawal, S. K. 2015. "Effect on Wrench-Feasible Workspace of Cable-Driven Parallel Robots by Adding Springs." *Mechanism and Machine Theory* 86: 201-10.

[5] Bosscher, P., Riechel, A. T., and Ebert-Uphoff, I. 2006. "Wrench-Feasible Workspace Generation for Cable-Driven Robots." *IEEE Transactions on Robotics* 22 (5): 890-902.

[6] Oh, S. R., and Agrawal, S. K. 2005. "Cable Suspended Planar Robots with Redundant Cables: Controllers with Positive Tensions." *IEEE Transactions on Robotics* 21 (3): 457-65.

[7] Fang, S., Franitza, D., Torlo, M., Bekes, F., and Hiller, M. 2004. "Motion Control of a Tendon-Based Parallel Manipulator Using Optimal Tension Distribution." *IEEE/ASME Transactions on Mechatronics* 9 (3): 561-8.

[8] Borgstrom, P. H., Jordan, B. L., Sukhatme, G. S., Batalin, M. A., and Kaiser, W. J. 2009. "Rapid Computation of Optimally Safe Tension Distributions for Parallel Cable-Driven Robots." *IEEE Transactions on Robotics* 25 (6): 1271-81.

[9] Oh, S. R., and Agrawal, S. K. 2006. "Generation of Feasible Set Points and Control of a Cable Robot." *IEEE*

Transactions on Robotics 22 (3): 551-8.

[10] LI, P. Y., and Horowitz, R. 1999. “Passive Velocity Field Control of Mechanical Manipulators.” *IEEE Transactions on Robotics and Automation* 15 (4): 751-63.

[11] Ros, L., Sabater, A., and Thomas, F. 2002. “An Ellipsoidal Calculus Based on Propagation and Fusion.” *IEEE Transactions on Systems, Man, and Cybernetics, Part B (Cybernetics)* 32 (4): 430-42.